Calculation of Shear Influences on the Phase Separation Behavior of Polymer Solutions in the Region of Their Lower Critical Solution Temperature. Creation of Closed Miscibility Gaps†

R. Horst and B. A. Wolf*

Institut für Physikalische Chemie der Universität Mainz, Jakob-Welder-Weg 13, D-6500 Mainz, Germany

Received April 23, 1990

ABSTRACT: Model calculations concerning the phase separation of sheared solutions were performed for a system with an exothermal Θ temperature of 333.3 K and 5000 polymer segments per chain. To determine the demixing conditions for a certain shear rate $\dot{\gamma}$, a generalized Gibbs energy $G_{\dot{\gamma}} = G_z + E_s$ was used. The Flory–Huggins equation, with a concentration- and temperature-dependent interaction parameter, served as an analytical expression for G_z, the Gibbs energy of mixing at zero shear. E_s, the energy that can be stored during stationary flow, as a function of composition, temperature, and $\dot{\gamma}$ was represented by typical empirical relations. The results of these calculations yield two peculiarities, which are typical for lower critical solution temperatures: (i) At some compositions a temperature interval of homogeneity separates the equilibrium solubility gap from a flow-induced region of immiscibility (bananalike extension of the equilibrium two phase area); this phenomenon is in accord with measurements reported in the literature. (ii) Under very special conditions the above-mentioned extension breaks away from the main heterogeneous region so that a closed miscibility gap is created; this prediction has so far not been verified experimentally.

Introduction

Polymer solutions and liquid polymer mixtures are in their phase-separation behavior sometimes very sensitive to shear or elongational forces, in contrast to low molecular weight systems. Early reports[1] on such effects date back to 1952, where shear-induced mixing was observed with solutions of two incompatible polymers in a common solvent. Since then numerous experimental and theoretical studies have been published on that subject.[2-20] All possible effects of flow can be observed: Depending on the molecular weight of the polymer, its concentration, and the applied shear rate or elongational speed, either shear dissolution or shear demixing turns up. For a given solution, the influences of flow can even change sign as the stress is increased. The theoretical reasons for this complex behavior are meanwhile well understood.[12]

Recently, a totally new phenomenon, namely, the occurrence of a very particularly shaped stress-induced two-phase region below a lower critical solution temperature (LCST) has been reported:[20] Within a certain range of compositions of the mixture one observes a temperature interval of homogeneity separating the equilibrium solubility gap from a flow-induced region of immiscibility. In the present contribution we will determine theoretically whether such behavior can be understood within the frame of the hitherto very successful model, in which the Gibbs energy of mixing is generalized by adding the energy a system can store while it flows. In addition, we have investigated whether further peculiarities associated with LCSTs can be predicted.

Theoretical Background

The starting point of the present calculations is eq 1[8] in which G_z is the Gibbs energy of mixing (zero shear,

$$G_{\dot{\gamma}} = G_z + E_s \tag{1}$$

equilibrium conditions) and E_s the energy a system can store in the stationary state while it flows. Since E_s constitutes in practically all cases of interest only a very small portion of G_z (normally less than 10^{-3}), the generalized Gibbs energy $G_{\dot{\gamma}}$ can be used to determine the conditions for the phase separation of flowing systems in the normal way. In the two subsequent sections it is shown how the two summands of eq 1 can be calculated.

Gibbs Energy of Mixing G_z. The thermodynamic properties of stagnant polymer solutions are described by

$$G_z/RT = x_1 \ln \varphi_1 + x_2 \ln \varphi_2 + g x_1 \varphi_2 \tag{2}$$

where G_z is the molar Gibbs energy of mixing; x_i and φ_i are the mole fraction and the volume fraction of the components (index 1 standing for the solvent and 2 for the polymer). With this relation, all characteristics of an actual system are incorporated into the (concentration- and temperature-dependent) interaction parameter g.

For the present calculations, g was expressed by[21]

$$g = \alpha + \beta_0/(1 - \gamma\varphi_2) \tag{3}$$

In this relation α and γ are constants for a given system and β_0 can in most cases be represented by

$$\beta_0 = \beta_{00} + \beta_{01}/T \tag{4}$$

From the above equations one obtains the following expressions[21] for the Θ temperature

$$\Theta = \beta_{01}[(0.5 - \alpha)/(1 - \gamma) - \beta_{00}]^{-1} \tag{5}$$

and for the critical point (index c)

$$2[\alpha + \beta_{0c}(1 - \gamma)/(1 - \gamma\varphi_{2c})^3] - 1/(N\varphi_{2c}^2) - 1/(1 - \varphi_{2c})^2 = 0 \tag{6}$$

and

$$6[\beta_{0c}\gamma(1 - \gamma)/(1 - \gamma\varphi_{2c})^4] + 1/(N\varphi_{2c}^2) - 1/(1 - \varphi_{2c})^2 = 0 \tag{7}$$

where N, the number of polymer segments, is calculated from the molar volumes V_i according to

$$N = V_2/V_1 \tag{8}$$

For the mathematical description of the equilibrium solubility gap of a certain polymer in a given solvent, the following four parameters are consequently required: α, β_{00}, β_{01}, and γ.

† Dedicated to Prof. R. Koningsveld on the occasion of his 65th birthday.

0024-9297/91/2224-2236$02.50/0

Stored Energy E_s. The energy E_s, which can be stored in 1 mol of a polymer solution during its stationary flow, is accessible[22] from measurements of the viscosity η as a function of shear rate $\dot{\gamma}$ according to

$$E_s = (x_1V_1 + x_2V_2)\eta\tau_0\dot{\gamma}^2(\eta/\eta_0)|\eta\dot{\gamma}|^{-2d^*} \quad (9)$$

η_0 is the zero shear viscosity and τ_0 the characteristic viscometric relaxation time, introduced by Graessley[23] for the description of flow curves by means of the following equations:

$$\eta/\eta_0 = g^{1.5}(\theta)h(\theta) \quad (10)$$

$$\theta = \eta/\eta_0\dot{\gamma}\tau_0/2 \quad (11)$$

$$g(\theta) = 2/\pi[\text{arccot}\,\theta + \theta/(1+\theta^2)] \quad (12)$$

$$h(\theta) = 2/\pi[\text{arccot}\,\theta + \theta(1-\theta^2)/(1+\theta^2)^2] \quad (13)$$

From experience one knows that τ_0 is normally on the order of the theoretically calculated Rouse relaxation time[24]

$$\tau_R = 6/\pi^2[(\eta_0 - \eta_s)M/(c_2RT)] \quad (14)$$

η_s is the viscosity of the pure solvent and c_2 the concentration (mass per volume) of the polymer with the molar mass M.

The parameter d^*, appearing in eq 9, constitutes a generalized power law exponent defined as

$$d^* = -(\partial \ln \eta)/(\partial \ln \dot{\gamma}) \quad (15)$$

and accounts for the fact that the ability of a solution to store energy becomes less as the disentanglement processes proceed. For known values of η_0 and τ_0, it can be calculated by means of eqs 10–13.

The temperature and concentration dependence of η_0 can frequently be described[25] by the Arrhenius eq 16, in which the parameters vary with φ_2 as formulated in eqs 17 and 18.

$$\ln(\eta_0/\text{Pa s}) = A + E^*/RT \quad (16)$$

$$A = A_0 + A_1\varphi_2 \quad (17)$$

$$E^* = E^*_0 + E^*_1\varphi_2 \quad (18)$$

For the mathematical description of E_s (at given M) as a function of composition, temperature, and shear rate, the following four parameters are required, as long as η_s can be neglected with respect to η_0 in eq 14: A_0, A_1, E^*_0, and E^*_1.

Calculation of Phase Diagrams

Mathematical Procedures. To determine the composition of phases′ and ″, which coexist in sheared systems, the double tangents to the function $G_{\dot{\gamma}}(x_2)$ (formerly constructed graphically[8]) were found by means of a computer. In other words, the calculator was programmed to search nonidentical x_2 values at which slope (eq 19) and

$$(\partial G_{\dot{\gamma}}/\partial x_2)' - (\partial G_{\dot{\gamma}}/\partial x_2)'' = f_1 = 0 \quad (19)$$

$$G_{\dot{\gamma}}(x_2') - (\partial G_{\dot{\gamma}}/\partial x_2)'x_2' - [G_{\dot{\gamma}}(x_2'') - (\partial G_{\dot{\gamma}}/\partial x_2)''x_2''] = f_2 = 0 \quad (20)$$

intercept (eq 20) of the tangents become identical. For the actual calculations a new function f was defined as

$$f(x_2',x_2'') = [(f_1^2 + f_2^2)/(x_2' - x_2'')^2]^{0.5} \quad (21)$$

which only becomes zero if eqs 19 and 20 are fulfilled and x_2' differs from x_2''. The solutions were found by an iteration program written in TURBO-Pascal on an IBM AT personal computer. The procedure OPT.LTD (simplex method) was purchased from Lauer & Wallwitz, Wiesbaden, Germany.

For the above calculations one requires an analytical expression for $E_s(x_2)$, one of the constituents of $G_{\dot{\gamma}}$. The best fit to experimental data and to theoretical values calculated by means of eq 9 was obtained with the following expression

$$E_s/RT = (c/a^2)\varphi_2^2\exp[-b(\varphi_2 - a)^2] \quad (22)$$

in which a, b, and c are parameters only depending on $\dot{\gamma}$ and T. For the discussion given in the next sections it is interesting to note that E_s passes a maximum at φ_2^{max} as the composition is varied at constant $\dot{\gamma}$. From $\partial E_s/\partial\varphi_2$ one obtains

$$\varphi_2^{max} = a/2 + (a^2/4 + 1/b)^{0.5} \quad (23)$$

By means of the equations formulated so far it is possible to calculate the phase diagrams for flowing liquid mixtures if the four thermodynamic and the four rheological parameters describing an actual system are known. How typical data for the LCSTs of present interest were selected is described in the next section.

Choice of Parameters. In order to model such systems, a reasonable value of N, i.e., molecular weight of the polymer, is selected. In the first step, experimental data of $\eta_0(\varphi_2,T)$, typical for moderately concentrated solutions of a polymer with N segments in thermodynamically poor solvents, are used to determine the parameters A_0, A_1, E^*_0, and E^*_1 in order to calculate $E_s(\varphi_2,T)$ for $\dot{\gamma}$ values of interest according to the eqs 9–15. The thus obtained data can then be represented by eq 22 after a, b, and c are fit.

The second step consists in the modeling of an equilibrium solubility gap by choosing the function $g(\varphi_2,T)$ within the range of values normally observed for LCSTs such that T_c is reasonable and that the shape of the coexistence curve agrees with experimental experience. The entire procedure is repeated for different values of N.

In the next section we investigate which combinations of the above parameters would lead to the so far theoretically inconceivable phenomenon of the shear-induced creation of a temperature interval of homogeneity separating two miscibility gaps mentioned in the Introduction.

Results and Discussion

For a qualitative assessment of shear effects on phase separation, the position and the shape of the plane $E_s(\varphi_2,T;\dot{\gamma})$ is decisive. Whether shear dissolution or shear demixing is observed depends on the curvature of this plane in the vicinity of the critical point of the stagnant solution, where the system is most sensitive against perturbances.

The occurrence of shear-induced phase separation, on which the present paper focuses, is closely bound to the relative position of the line $\varphi_2^{max}(T;\dot{\gamma})$ [projection of the maximum of $E_s(\varphi_2,T;\dot{\gamma})$ into the plane of the phase diagram] and the critical point of the system. This is because the phases that coexist at a given temperature and shear rate in the formerly homogeneous region are situated below and above φ_2^{max}, respectively.

Suitable Combinations of Parameters. To realize shear demixing theoretically, one determines the range of the number of segments N for which the above conditions can be fulfilled *with reasonably large shear rates*. For $\dot{\gamma}$ it is necessary to exceed a certain minimum value to ensure that E_s becomes large enough to perturb $G_z(x_2)$ in a way

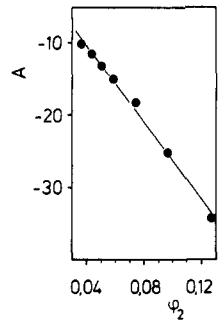

Figure 1. Concentration dependence of the Arrhenius parameter A, eq 16, describing the temperature influence on the zero shear viscosity of polymer solutions representative for the present model system, as obtained from evaluation of literature data.[25] φ_2 is the volume fraction; the concentration influences are given by eq 17 with $A_0 = 0.390$ and $A_1 = -267$.

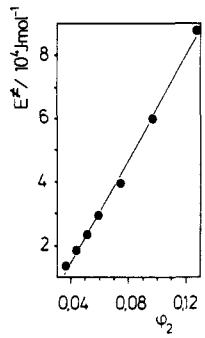

Figure 2. Concentration dependence of the Arrhenius parameter E^*, eq 16, describing the temperature influence on the zero shear viscosity of polymer solutions representative for the present model system, as obtained from evaluation of literature data.[25] φ_2 is the volume fraction; the concentration influences are given by eq 18 with $E^*_0 = -0.179\ 10^5$ J/mol and $E^*_1 = 8.15\ 10^5$ J/mol.

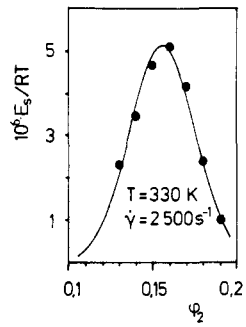

Figure 3. Reduced stored energy E_s/RT (T = 330 K) of the present model system as a function of φ_2, the volume fraction of polymer, for a constant shear rate of 2500 s^{-1}. The data points are calculated by means of eqs 9–15; the curve is fitted as formulated in eq 22.

that creates two phases where the stagnant system is homogeneous. $N = 5000$ turned out to be the best choice for the model system; V_1 was set at 100 cm^3/mol.

The viscosity data required for the calculation of E_s were taken from ref 25 for almost the same N value and the system 2-propanol/poly(*n*-butyl methacrylate). $\eta_0(T,\varphi_2)$ is documented in Figures 1 and 2 in terms of the concentration dependence of the Arrhenius parameters eqs 16–18, which are given numerically in the legends to the figures. The quoted relations only hold true for $\varphi_2 > 0.035$.

An example for the reduced stored energy E_s/RT calculated by means of the above relations and eqs 9–15 for different concentrations is given in Figure 3 for a shear rate $\dot{\gamma}$ of 2500 s^{-1} together with the curve fitted to these points according to eq 22.

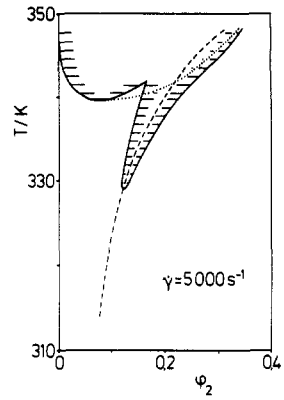

Figure 4. Phase diagram calculated for the model system at zero shear (dotted line) and at 5000 s^{-1} (full line). The broken line gives the temperature dependence of the composition at which the stored energy becomes maximum for the above shear rate [$\varphi_2^{max}(T)$, cf. eq 23].

The following thermodynamic parameters (lying all within the range observed with actual systems) were chosen to describe the phase-separation behavior of the stagnant model system: $\alpha = 0.174$, $\beta_{00} = 0.862$, $\beta_{01} = -70$ K, and $\gamma = 0.50$. To find these values, a comparatively large γ (in order to extend the sensitive region existing in the vicinity of the critical point with respect to composition) and a comparatively low $|\beta_{01}|$ (to extent this area with respect to temperature) were selected. The remaining two parameters were then adjusted to fix the critical point of the model system in a reasonable position, namely, at $\varphi_{2c} = 0.09$ and $T_c = 339.7$ K ($\Theta = 333.3$ K).

We are now in a position to calculate phase diagrams for the flowing model system at different shear rates and to investigate in which way the behavior near LCSTs differs from that near upper critical solution temperatures (UCSTs).

General Phenomena. The behavior depicted in Figure 4 shows the present model system at high shear rates. It is characterized by the cooccurrence of shear dissolution and shear demixing. For instance, for $\varphi_2 = 0.15$ and a temperature close to the phase-separation temperature of the stagnant system, a shear rate of 5000 s^{-1} increases the homogeneous region, whereas it produces a solubility gap with a width of ca. 5 K at lower temperatures, where the system is one phase at rest. The territory of additional heterogeneity created by shear emerges from the equilibrium two-phase region and centers around the curve $\varphi_2^{max}(T)$ also shown in this graph (eq 23). The features of shear dissolution resemble closely that observed with UCSTs, in particular one also finds an eulytic point (coexistence of three liquid phases, cf. ref 8).

The situation depicted in Figure 4 is very similar to that reported[20] for mixtures of two polymers differing considerably in chain length: Keeping the polymer concentration constant, the authors have also observed a temperature interval of homogeneity separating two miscibility gaps. For some reason they have, however, not observed the reentry into the homogeneous region upon further lowering T, which, however, has to take place inevitably, except for those cases where an UCST is close enough.

Creation of Closed Miscibility Gaps. Keeping all parameters of the model system constant, but halving the shear rate to a value of 2500 s^{-1}, leads to the phase diagram shown in Figure 5. Under these conditions the degree of shear dissolution results somewhat less and the eulytic point vanishes.

The most prominent feature, however, is the shear-induced occurrence of an additional, closed two-phase region with an extent of almost 20 K and an upper limit

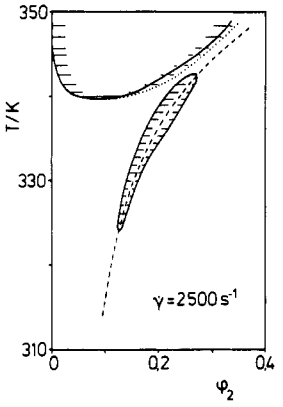

Figure 5. Phase diagram calculated for the model system at zero shear (dotted line) and at 2500 s^{-1} (full line). The broken line gives the temperature dependence of the composition at which the stored energy becomes maximum for the above shear rate.

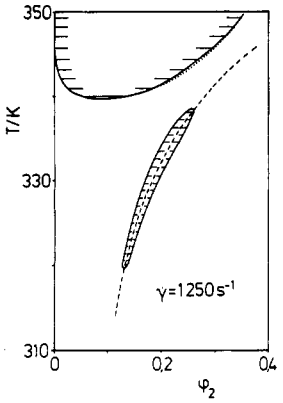

Figure 6. Phase diagram calculated for the model system at zero shear (dotted line) and at 1250 s^{-1} (full line). The broken line gives the temperature dependence of the composition at which the stored energy becomes maximum for the above shear rate.

somewhat above T_c. To our knowledge, no such a behavior has been observed so far.

As already mentioned, the heterogeneous domain is in its position fixed by $\varphi_2^{max}(T)$. The explanation for the segregation of this two-phase region from the rest of the solubility gap lies in the fact that this curve, unlike that for the higher shear rate (Figure 4), passes the equilibrium solubility gap without intersecting it.

On a renewed halving of the shear rate to a value of 1250 s^{-1}, $\varphi_2^{max}(T)$ is again shifted toward higher concentrations and consequently the amount of shear dissolution and of shear demixing is further diminished. As can be seen from Figure 6, the equilibrium solubility gap remains almost unchanged by shear and the lateral dimension of the shear-induced additional closed two-phase region has almost vanished.

Comparison of Shear Effects near LCSTs and UCSTs. As already briefly indicated above, the phenomena of shear dissolution (including the possibility of eulytic points) and of shear demixing (in the sense of a simple extension of the equilibrium solubility gap) are common to both types of critical temperatures. There exists, however, one important particularity with LCSTs, namely, the possibility of creating closed solubility gaps in an area where the system is homogeneous at rest.

The theoretical explanation for this behavior is twofold. First, the miscibility increases for a LCST as T is lowered, whereas it decreases for an UCST. However, in both cases a reduction of T increases η_0 and consequently E_s, the energy that can be stored in the system. This situation makes the temperature region slightly below a LCST particularly sensitive to shear influences. Second, the curve $\varphi_2^{max}(T)$ (which governs the position of additional two-phase regions) can pass the solubility gap associated with a LCST without intersecting it, whereas this is obviously practically impossible with UCSTs. Since the absence of such a crossing point is a necessary condition for the occurrence of a shear-induced closed miscibility gap, it can be rationalized why that phenomenon is restricted to LCSTs.

Outlook

Although the present calculations have been performed with a model system and only for polymer solutions that are sheared, it can be anticipated that the results are qualitatively also applicable to polymer mixtures and to extensional flow. In the case of polymer mixtures, it is expected that the effects are even larger because of the increased amounts of energy that can be stored and as a consequence of a lesser concentration dependence of the chemical potential of the components in the vicinity of the critical point. Similarly, it can be anticipated that the qualitative features remain the same, no matter whether the energy is stored via shearing or elongational forces.

Naturally one has to verify the results of the present model calculations, which indicate the possible occurrence of closed miscibility gaps in the vicinity of LCSTs and the above-mentioned speculations concerning other types of systems or stresses. Corresponding experiments with LCSTs and polymer/solvent systems are planned, as are additional theoretical calculations for polymer mixtures and extensional flow.

Acknowledgment. We are grateful to the Deutsche Forschungsgemeinschaft for the support of this work. We also thank Prof. H. H. Winter for making his typescript[20] available to us prior to publication.

References and Notes

(1) Silberberg, A.; Kuhn, W. *Nature (London)* **1952**, *170*, 450.
(2) Breitenbach, J. W.; Wolf, B. A. *Makromol. Chem.* **1968**, *117*, 163.
(3) ver Strate, G.; Philipoff, W. *J. Polym. Sci., Polym. Lett. Ed.* **1974**, *12*, 267.
(4) Wolf, B. A.; Jend, R. *Macromolecules* **1979**, *12*, 732.
(5) Schmidt, J. R.; Wolf, B. A. *Colloid Polym. Sci.* **1979**, *257*, 1188.
(6) Wolf, B. A. *Makromol. Chem., Rapid Commun.* **1980**, *1*, 231.
(7) Perez-Garcia, C.; Jou, D. *Phys. Lett.* **1983**, *95A*, 23.
(8) Wolf, B. A. *Macromolecules* **1984**, *17*, 615.
(9) Rangel-Nafaile, C.; Metzner, A. B.; Wissbrunn, K. F. *Macromolecules* **1984**, *17*, 1187.
(10) Krämer, H.; Wolf, B. A. *Makromol. Chem., Rapid Commun.* **1985**, *6*, 21.
(11) Onuki, A. *Phys. Rev. A* **1986**, *34*, 3528.
(12) Krämer-Lucas, H.; Schenck, H.; Wolf, B. A. *Makromol. Chem.* **1988**, *189*, 1613, 1627.
(13) Rector, L. P.; Mazich, K. A.; Carr, S. H. *J. Macromol. Sci., Phys.* **1988**, *B27*, 421.
(14) Cheikh Larbi, F. B.; Malone, M. F.; Winter, H. H.; Halary, J. L.; Leviet, M. H.; Monnerie, L. *Macromolecules* **1988**, *21*, 3532.
(15) Lyngaae-Jørgensen, J. *Polym. Mater. Sci. Eng.* **1988**, *58*, 702.
(16) Nakatani, A. I.; Kim, H.; Takahashi, Y.; Han, C. C. *Polym. Commun.* **1989**, *30*, 143.
(17) Bhattacharjee, S. M.; Fredrickson, G. H.; Helfand, E. *J. Chem. Phys.* **1989**, *90*, 3305.
(18) Takebe, T.; Sawaoka, R.; Hashimoto, T. *J. Chem. Phys.* **1989**, *91*, 4369.
(19) Hess, S.; Loose, W. *Ber. Bunsenges. Phys. Chem.* **1990**, *94*, 216.
(20) Katsaros, J. D.; Malone, M. F.; Winter, H. H. *Polym. Eng. Sci.* **1989**, *29*, 1434.
(21) Koningsveld, R.; Kleintjens, L. A. *Macromolecules* **1971**, *4*, 637.
(22) Wolf, B. A. *Markomol. Chem., Rapid Commun.* **1987**, *8*, 461.
(23) Graessley, W. W. *Adv. Polym. Sci.* **1974**, *16*, 1.
(24) Rouse, P. E. *J. Chem. Phys.* **1953**, *21*, 1272.
(25) Herold, F. K. Dissertation, University of Mainz, 1985.